

SPATIALLY RESOLVED PROPERTIES OF THE GRB 060505 HOST: IMPLICATIONS FOR THE NATURE OF THE PROGENITOR

Christina C. Thöne¹, Johan P. U. Fynbo¹, Goran Ostlin², Bo M. Ilvang-Jensen¹, Klaas Wiersema³, Daniele Malesani¹, Desiree Della Valle⁴, Monica Ferreira¹, Javier Gorosabel⁴, D. Alexander Kann⁵, Darach Watson¹, Michał J. Michałowski¹, Jens Hjorth¹, Andrew S. Fruchter⁶ and Jesper Sollerman^{1,2}

Draft March 2007

ABSTRACT

GRB 060505 was the first well-observed nearby long-duration GRB that had no associated supernova. Here we present spatially resolved spectra of the host galaxy of GRB 060505, an Sbc spiral, at redshift $z = 0.0889$. The GRB occurred inside a star-forming region in the northern spiral arm at 6.5 kpc from the center. From the position of the emission lines, we determine a maximum rotational velocity for the galaxy of $v = 212 \text{ km s}^{-1}$ corresponding to a mass of $1.3 \cdot 10^{11} \text{ M}_\odot$ within 24 kpc. The H α equivalent width at the GRB site gives a very young age of $< 7 \text{ Myr}$. By fitting single-age spectral synthesis models to the stellar continuum, we derive ages for the dominant stellar populations in different parts of the galaxy resulting in $> 800 \text{ Myr}$ for the bulge and only $< 35 \text{ Myr}$ for the GRB site. The metallicity derived from the R_{23} parameter is lowest at the GRB site with $0.14 Z_\odot$ but roughly solar in the rest of the galaxy. The extinction in the galaxy is overall low with $A_V < 0.40 \text{ mag}$ in the bulge and $A_V < 0.09 \text{ mag}$ at the GRB site. Using the 2dF galaxy redshift survey we can locate the host galaxy in its large scale (Mpc) environment. The galaxy lies in the foreground of a filamentary overdensity extending southwest from the galaxy cluster Abell 3837 at $z = 0.0896$. The properties of the GRB site are similar to those found for other long-duration GRBs with high specific star formation rate and low metallicity, which is an indication that GRB 060505 originated from a young massive star that died without making a supernova.

Subject headings: Gamma rays: Bursts: Individual: GRB 030329, GRB host galaxies, SN-less GRB

1. INTRODUCTION

GRB 060505 reinitiated the discussion on the connection between long gamma-ray bursts (GRBs) and core-collapse supernovae (SNe) as established with the detection of a SN spectrum in the afterglow of GRB 030329 (Hjorth et al. 2003; Stanek et al. 2003). Despite intense photometric and spectroscopic searches, no sign of a SN was detected for the nearby GRBs 060505 and 060614 (Fynbo et al. 2006; Gal-Yam et al. 2006; Della Valle et al. 2006). This raised the question of whether all long GRBs are accompanied by SNe (Zeh et al. 2004) or whether our understanding of the explosion mechanism is incomplete (Gehrels et al. 2006; Fryer, Young & Hungerford 2006; King et al. 2007; Zhang et al. 2007).

The Swift satellite (Gehrels et al. 2004) detected GRB 060505 on May 5 2006, 06:36:01 UT, which had a fluence of $(6.2 \pm 1.1) \cdot 10^{-7} \text{ erg cm}^{-2}$ (Hullinger et al. 2006). With a duration of $T_{90} = 4 \text{ s}$ it falls in the class of

Based on ESO-TOO proposal 077.D-0661 and ESO-LP proposal 177.A-0591

Electronic address: cthoene@dark-cosmology.dk

¹ Dark Cosmology Centre, Niels Bohr Institute, University of Copenhagen, Juliane Maries Vej 30, 2100 Copenhagen, Denmark

² Stockholm Observatory, Department of Astronomy, AlbaNova, S-106 91, Stockholm, Sweden

³ Astronomical Institute 'Anton Pannekoek', University of Amsterdam, Kruislaan 403, 1098 SJ Amsterdam, The Netherlands

⁴ Instituto de Astrofísica de Andalucía (IAA-CSIC), P.O. Box 3.004, E-18.080 Granada, Spain

⁵ Thüringer Landessternwarte Tautenburg, Sternwarte 5, D-07778 Tautenburg, Germany

⁶ Space Telescope Science Institute, 3700 San Martin Drive, Baltimore, Maryland 21218, USA

long-duration GRBs. The satellite did, however, not slew automatically as the GRB was too faint to be detected on-light (Palm et al. 2006). One of the two sources inside the BAT error circle detected by the XRT was finally established to be fading (Conciatore et al. 2006), thereby localizing GRB 060505 to a region 4° north of the center of the 2dFGRS spiral galaxy TG S173Z112 at a redshift of $z = 0.089$. An optical afterglow (Ofek et al. 2006) was found 1° from the center of the revised XRT error circle with a radius of 2° (Butler 2007). Later imaging and spectroscopy established the burst position to be coincident with a bright, compact star-forming region in one of the spiral arms of the host galaxy (Thöne et al. 2006a; Fynbo et al. 2006), which was revealed to be a late-type, strong emission line galaxy from the 2dFGRS data (Colless et al. 2001).

Host galaxies of GRBs are usually too distant to allow spatially resolved analysis with ground-based observations. Therefore, we only have informations on the global properties of the galaxies, which appear to be mostly young, irregular, star-forming dwarf galaxies (Le Floc'h et al. 2003; Christensen et al. 2004). However, we know very little about the properties of the actual explosion sites. A recent study of GRB hosts observed with the HST (Fruchter et al. 2006), which spatially resolved the host galaxies of 42 long GRBs, showed that the explosion sites coincide with the brightest regions in their host galaxies. Only two GRB hosts could so far be well resolved from the ground, those of GRB 980425 (Sollerman et al. 2005) and GRB 020819 (Jakobsson et al. 2005), both being spiral galaxies. In both cases, the GRBs occurred close to H II regions in the spiral arms of their host galaxies which supports the

connection between long GRBs and the deaths of massive stars.

In this paper, we present deep observations of the host galaxy of GRB 060505 in order to compare the galaxy and the burst site with the host galaxies of other long GRBs and to explicate the controversial nature of this SN-less long duration GRB. In Sect. 2, we present spatially resolved spectroscopy of the host galaxy as well as photometric data. Sect. 3 describes the general properties of the galaxy, concerning the classification, photometry of the entire galaxy, colors, mass determination as well as dynamical measurements. In Sect. 4, we examine the differences between several parts of the galaxy including the GRB site, the different stellar populations and their ages as well as differences in metallicity and extinction along the galaxy. The last section, finally, studies the large scale structure around the host galaxy.

Throughout the paper we adopt a cosmology with $H_0 = 71 \text{ km s}^{-1} \text{ Mpc}^{-1}$, $m = 0.27$, $\Omega = 0.73$. A redshift of $z = 0.0889$ then corresponds to a luminosity distance of 401 Mpc and 1° corresponds to 1.64 kpc.

2. OBSERVATIONS

Spectra were taken with FORS2 at the Very Large Telescope (VLT) on Cerro Paranal in Chile on May 23, 2006, 18 days after the burst when there was no contribution from the afterglow. We used grism 300V, which covers the wavelength range 3500–9600 Å, and a 1° wide slit resulting in a resolution of 11 Å full width at half maximum (FWHM) or 650 km s⁻¹ at $\lambda = 5600 \text{ Å}$. Seeing conditions were decent with a DIMM seeing of 0.89 FWHM. In order to minimize the effects of atmospheric dispersion, the FORS instrument uses a so called "Longitudinal Atmospheric Dispersion Corrector" (LADC) which reduces differential slit loss. We obtained two 1800 s and one 600 s exposures which were combined and reduced with standard packages in IRAF. The dispersion solution used for the wavelength calibration had an RMS of about 0.1 Å.

The coadded 2D spectrum was divided into four pieces of eight and one piece of nine pixels width along the spatial direction, where 1 pixel corresponds to 0.25 or 0.41 kpc at the redshift of the galaxy. These five parts represent distinct regions in the galaxy such as the spiral arms and the GRB site covered by the slit (see Figures 1, 2 and also Fig. 4). We used the continuum of the bulge which has the brightest trace to create a "tem plate" trace and extract all five pieces using the same trace function, in order to account for the bending of the trace towards the blue. The individual parts were then flux calibrated with IRAF using observations of the spectrophotometric standard star LTT 7379 from 2006 April 2 which was taken under photometric conditions. Cross-calibration with observations of the standard star LTT 1788 on August 17 gave consistent results for the fluxes. We estimate the error of the flux calibration to be around 10% in the wavelength range between 4000 and 7500 Å which covers the range of the host galaxy emission lines. The flux calibration obtained in such a way can, however, only serve as a relative flux calibration and to determine the shape of the continuum.

Imaging was obtained with FORS1 at the VLT in the BVRIZ bands on 2006 September 14 and in U on 2006

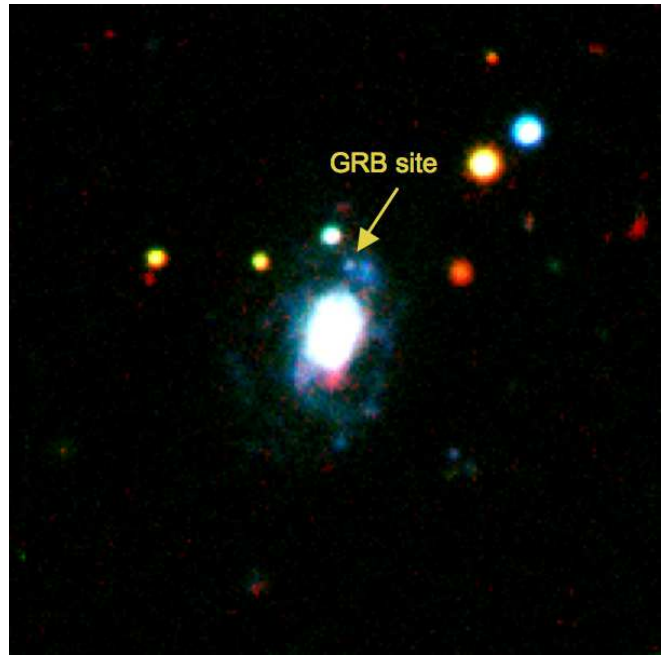


Fig. 1. | Color picture of the host galaxy of GRB 060505 from B, R, Ks bands, field of view $40'' \times 40''$, North up, East left. The position where the OT occurred is marked.

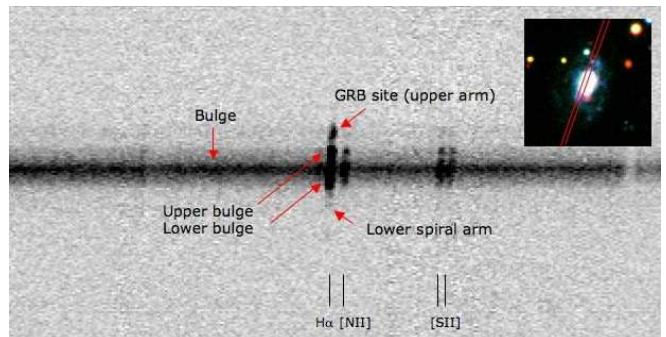


Fig. 2. | 2D longslit spectrum of the host galaxy of GRB 060505 around the H_α emission line. Indicated are the 5 parts that were extracted from the spectrum. The inset shows the position of the slit across the host galaxy.

October 1 under photometric conditions. Images in the Ks band were taken with ISAAC at the VLT on September 24. The images of FORS1/VLT in UBVRI were calibrated using photometric zeropoints from the same night as the observations in the corresponding bands. For the z band which has no zeropoints available, we calibrated a standard field observed on the same night with magnitudes from SDSS observations of the same field, which was then used to derive instrumental zeropoints in the z-band. The K band image was calibrated using a comparison star in the same field from the 2MASS catalogue.

3. GLOBAL PROPERTIES OF THE GALAXY

3.1. Classification

The host galaxy of GRB 060505 is a late-type spiral galaxy with at least two major spiral arms, where the GRB occurred in the northern arm (see Fig. 1). From the morphology and from the strength of the H_α, H_β and the forbidden nebular emission lines (see Sect. 4), this galaxy can be classified as an Sbc spiral (Kennicutt 1992a). We

TABLE 1
Photometry of the host galaxy

Filter	m _{mag}	color	m _{mag}
U	18.43	0.05	
B	18.89	0.02	U B 0.46 0.05
V	18.27	0.02	B V 0.62 0.03
R	17.90	0.02	V R 0.37 0.03
I	17.51	0.02	R I 0.39 0.03
z	17.29	0.08	R z 0.59 0.08
K	15.85	0.04	R K 2.05 0.04

Note. | M magnitudes given are in the Vega system. The values are corrected for the foreground extinction of $A_V = 0.06$

detect Ca H & K absorption lines and the 4000 Å break, Ca H is, however, only clearly detected in the bulge region. The three other spiral host galaxies of long GRBs had also been late-type spiral galaxies with GRB 980425 occurring in an SBc spiral (Fynbo et al. 2000), 990705 in an Sc (Le Floc'h et al. 2002) and GRB 020819 possibly in an SB spiral galaxy (Jakobsson et al. 2005).

We determined the magnitudes of the entire host galaxy using the images in UBVRI from FORS/VLT and in K from ISAAC. In order to get the total flux of the host galaxy, apertures of $15''$ were used for the U band, $12''$ for BVRIZ and $8''$ for the K band which were the smallest sizes to contain the total flux. The flux of the three stars inside the apertures contributing about 10% to the total flux was removed. These magnitudes and the corresponding colors are listed in Table 1, the magnitudes are corrected for the foreground extinction of $A_V = 0.06$. From the R-band magnitude we derive an absolute magnitude for the host of $M_R = -20.15$ 0.02 mag which corresponds to $0.4 L/L^*$ with $M_R^* = -21.21$ mag (Blanton et al. 2001) using $h = 0.7$. The colors of this galaxy are actually too blue for an Sbc spiral galaxy but rather resemble the values for an irregular galaxy (Fukugita et al. 1995). Also the equivalent widths (EW) of the emission lines are generally stronger than expected for a normal Sbc spiral (Kennicutt 1992b).

A closer look at the morphology reveals some distortion from the regular spiral structure which can also be seen in the HST images of the host galaxy presented in O’Fek et al. (2007). The upper and lower major spiral arms seem not to lie symmetrically around the central bulge region. In addition, there seems to be an additional structure on the western side of the bulge. This suggests a recent minor merger event which could have triggered the excess star formation in parts of the host that has overall an older population (see Sect. 4.3). It might also explain the deviation of the colors and emission line strengths compared to usual Sbc spiral galaxies.

3.2. Measurement of the rotation curve

In order to measure the rotation curve of the host galaxy, the four brightest emission lines in the 2D spectrum were used, namely [O ii], H α , [O iii] and H β . A 2D continuum subtracted postage stamp spectrum was produced for each emission line, with the continuum being modelled as a linear function fitted near each emission line. For each spatial point along the slit, the postage stamp spectrum, a Gaussian was fitted using the IRAF task `ngaussfit` from the STSDAS package. At first

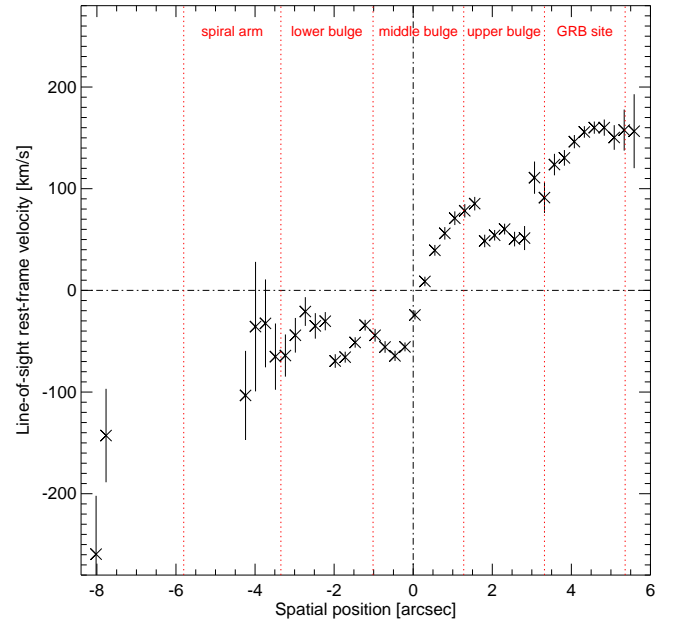


Fig. 3. | Rotation curve using the weighted mean of the center of the emission lines [O ii], H α , [O iii] and H β over the spatially resolved host galaxy spectrum.

the FWHM was kept as a free parameter, resulting in a typical value of 9 Å. The FWHM was then fixed at 9 Å, and a Gaussian was fitted again to each row, now with only two free parameters, the center (i.e. observed wavelength) and amplitude. Uncertainties on the fitted parameters were calculated using `ngaussfit` based on an input noise spectrum which was calculated as photon noise and read-out noise from the 2D galaxy spectrum before sky subtraction.

The fitted observed wavelengths were first corrected for a zero point error in the wavelength calibration. The fitted observed wavelengths λ_{obs} were then used to calculate rest-frame line-of-sight velocities as $v_{\text{rest}}^{\text{los}} = c(z - z_{\text{sys}})/(1 + z_{\text{sys}})$, with $z = \lambda_{\text{obs}} - \lambda_{\text{rest}} = 1$ where a systematic redshift of $z_{\text{sys}} = 0.0889$ was used. ‘Line-of-sight’ means that no correction for inclination has been applied. The row number in each postage stamp spectrum was transformed into a spatial coordinate with respect to the continuum center. The location of the continuum center as a function of observed wavelength (the ‘trace’ of the continuum) was measured in a number of bins in an aperture of width 14 pixels = $3''$ and fitted using a linear function. The used systematic redshift was chosen so that the median velocity of the 16 data points (4 per emission line) located within $0''$ of the continuum center was zero. In other words, the calculated velocities were defined to be zero at the continuum center.

To plot the rotation curve we only use points for which the fitted Gaussian amplitude was larger than three times its uncertainty. The rotation curves based on the 4 emission lines agreed reasonably well, although there were places where the difference was larger than what the calculated uncertainties could explain. The weighted mean rotation curve shown in Fig. 3 was calculated using inverse variance weighting.

3.3. Galaxy size and mass

In order to determine the inclination of the galaxy, we measured the ellipticity of the disc with SExtractor (Bertin & Arnouts 1996) using the photometric data in the V, R and I bands. We find $e = 0.346 \pm 0.006$ which gives an inclination of 49 ± 1 degrees. The half-light diameter of the galaxy disc is about $11''$ which corresponds to a line-of-sight diameter of 18.05 kpc or a diameter of 24 kpc, taking into consideration the inclination of 49 degrees.

From fitting empirical models for GRB host galaxies according to Michałowski & Jordt (2007) to the spectral energy distribution (SED) of the galaxy, we can also determine the total stellar mass to $(7.9 \pm 0.4) \times 10^9 M_{\odot}$ and the total baryonic mass being two times the stellar mass. The error quoted comes only from the errors of the model fitting, the total error from the model itself is around a factor of two. The measurement of the rotation curve which attains at a value of 160 km s^{-1} (line-of-sight) or 212 km s^{-1} (considering the inclination) allows another rough estimate of the total galaxy mass to $1.3 \times 10^{11} M_{\odot}$ taking the half-light radius of 12 kpc. The mass value derived from the rotation curve, however, also includes the dark matter whereas the value from the SED fitting delivers only the baryonic mass.

4. SPATIALLY RESOLVED PROPERTIES

Fig. 4 shows the different regions selected for the analysis of the properties in different parts of the galaxy. The three peaks in H α within the bulge seem to come from the nucleus of the galaxy and the innermost regions of the two spiral arms as can be seen in the color picture (Fig. 1). The region in the upper spiral arm around the site where the GRB occurred is a large H II region, representing a clear peak in the H α spatial profile. A second H II region is to the west of the GRB position, just outside the slit. The spiral arm below the bulge only has a very weak peak in H α , which indicates a low star formation rate in this region.

We analyze the properties of the ISM in the individual regions by comparing the emission line fluxes from the different regions (see Table 2). The Balmer lines H α , H β and H γ were found in emission in all regions, except that H γ was not detected in the faint spectrum of the lower spiral arm. We also detect the forbidden lines [O III] 3727,3729 and [O III] 5007,4959 as well as [N II] 6568 and the [S II] 6716,6731 doublet. We measured the line properties (see Table 2) using the splot task in IRAF which fits gaussians to the lines. The lines are unresolved within the resolution of the instrument.

The detection of several bright forbidden emission lines allows us to evaluate the possibility of an Active Galactic Nucleus (AGN) contribution to the excitation of the nebular lines. Kauffmann et al. (2003) analysed a large sample of SDSS galaxy spectra to empirically find the demarcation between starburst galaxies and AGNs as follows: a galaxy is AGN dominated if

$$\log([O\ III] 5007/H\ \beta) > \frac{0.61}{\log([N\ II]/H\ \beta)} + 1.3 \pm 0.05$$

whereas we get 0.20 ± 0.02 for the left side of the equation and 0.46 ± 0.03 using the extinction corrected line fluxes for the bulge region which clearly disfavours an AGN contribution. Hence we assume that the host

galaxy nebular emission line excitation is not dominated by (non-thermal) AGN emission.

4.1. Burst location

In a few bursts, where the position of the GRB within the host galaxy could be determined accurately, the burst seemed not to be within the regions with the highest star formation (Hammer et al. 2006) nor the bluest parts (Fruchter et al. 2006). For XRF 020903 it was shown that the GRB occurred close, but not inside, a massive, star-forming supercluster (Le Floc'h et al. 2006; Fruchter et al. 2006). GRB 980425 also had an offset of 460 pc from a compact star-forming region (Hammer et al. 2006), it was, however, coincident with a smaller star-forming region (Fynbo et al. 2000; Sollerman et al. 2002).

We investigated the location of GRB 060505 within the host galaxy where we compared the OT position from the image subtraction in the FORS R-band with the position of the H II region in the image of the galaxy used as subtraction template (Fynbo et al. 2006). From that analysis, we find that the centroid of the afterglow and the H II region coincide to within 0.1 or 40 pc in projection. HST images from the host galaxy (Olefki et al. 2007) also show clearly that the burst lies at the edge of an H II region with a size of 400 pc. Therefore, it seems unlikely that GRB 060505 was a chance superposition with the galaxy and in fact occurred at a higher redshift, which could have been an explanation for the lack of the detection of a SN. This clear association of the OT position with a star-forming region also strengthens the suggestion that GRB 060505 was due to the collapse of a massive star that originated in this star-forming region.

4.2. Extinction

Another issue in the discussion about the missing SN in the lightcurve of GRB 060505 was the argument of extinction in the line of sight. The Galactic extinction along the line of sight of the GRB determined from the sky maps of Schlegel et al. (1998) is very low with $E(B-V) = 0.021$ mag, for which the entire spectra are corrected. In order to get the extinction in the different parts in the host galaxy, we used the Balmer line decrement which should give values of $H\beta/H\alpha = 2.73$ for no extinction, assuming $T = 10000\text{K}$ and case B recombination (Osterbrock 1989). Before deriving the Balmer line decrement, we corrected the Balmer emission lines for the absorption from the different underlying stellar populations from the models as described in Sect. 4.3. The values of the Balmer absorption are also noted in Table 2.

The Balmer line decrement analysis shows that there is not much extinction throughout the galaxy which is not unexpected as we see the galaxy close to face-on. There seems to be some extinction in the bulge region as well as at the GRB site where we infer upper limits of $A_V < 0.40$ mag and $A_V < 0.09$ mag. The emission lines in these two parts are corrected for the extinctions found using a MW extinction law (Cardelli et al. 1989). We note that the very low extinction derived for the GRB site clearly disfavours the possibility of having missed an underlying SN due to extinction or the GRB being inside a dense part of the SF region.

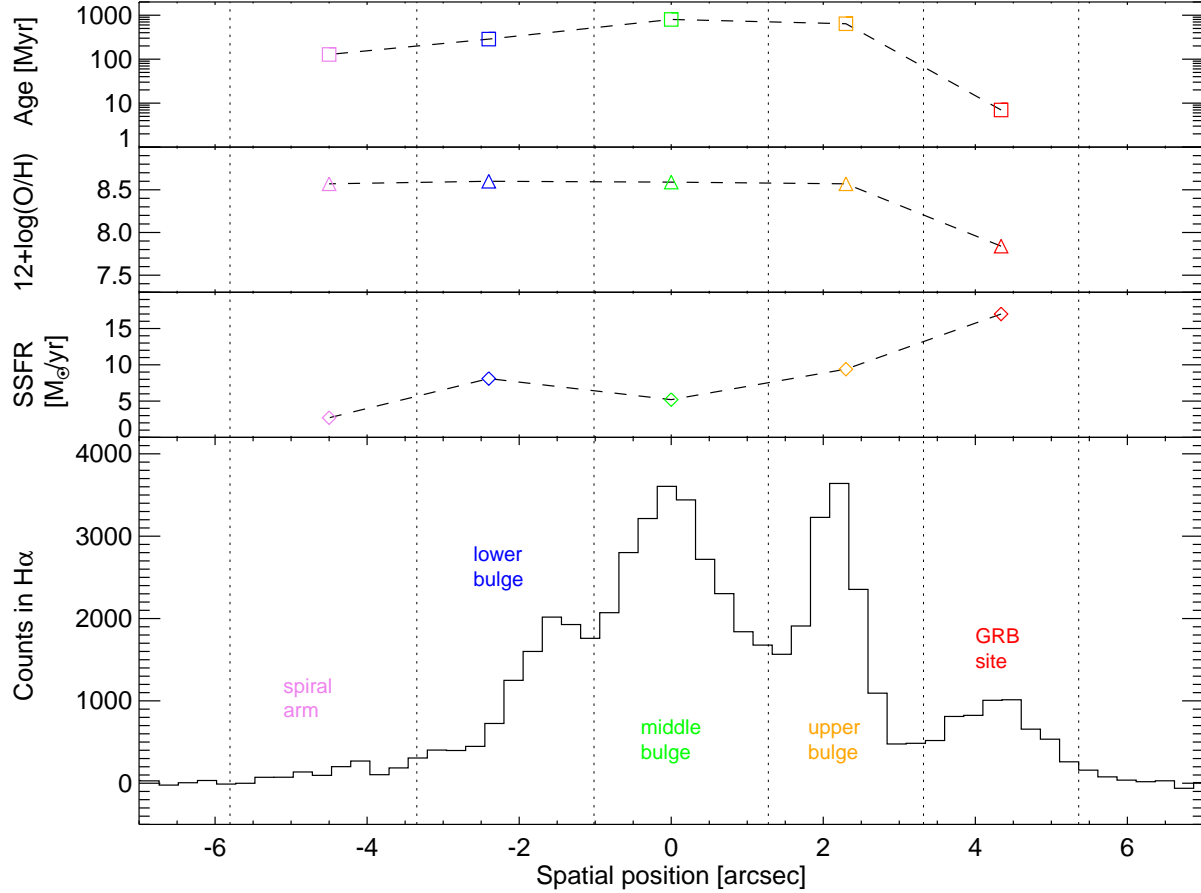


Fig. 4.1 Lower panel: Cut through the spectrum along the H α line and indication of the regions selected for the individual spectra. The same regions are plotted in the inset R band in age of the galaxy, which also shows the position of the slit. The upper three panels show the $12+\log(O/H)$ metallicity, the specific SFR per luminosity and the age of the stellar population in the five parts of the spectrum indicated in the H α plot. The errors of the values plotted are within the size of the datapoints. All three panels show that the GRB site is considerably different from the rest of the host galaxy.

We also determined the extinction from the broadband afterglow photometry using the values of the afterglow from the series of observations in the B, V, R and I bands from the first night with the contribution of the galaxy subtracted (D. Xu et al. in preparation). The SED gives no indication of additional reddening along the line of sight through the galaxy and the slope is consistent within the errors to the X-ray data from the Swift XRT observations. This rules out the possibility that GRB 060505 was obscured by dust which would have prevented the detection of a SN. The low extinction might also provide further evidence that the burst did not take place at higher redshift, though we have no information about the total extinction through the disc of that galaxy.

4.3. Stellar population modeling

In order to characterize the ages of the dominant stellar populations in the different parts of the host, the GRB site and the entire galaxy, we used several different methods. From fitting the spectral energy distribution (SED) of the entire galaxy (Bolzonella, Miralles & Pello 2000) using the photometric values from Table 1, we get a generally old population of 9.5 G yr with solar metallicity and no extinction. A better determination would

be possible with J and H band data available.

One indicator for the age of a population, especially when it is very young, is the predicted evolution of the H α EW derived from the spectra. Assuming an Salpeter IMF from 0.08 to 120 M \odot and a metallicity of $Z = 0.004$ or $12+\log(O/H) = 8.27$ which is close to the spectroscopically determined value, the EW of 180 Å indicates an age of 7 ± 1 M yr or less according to the evolution of the EW derived by Zackrisson et al. (2001). This value has to be interpreted as an upper limit due to the H I covering factor leading to a possible Lyman continuum leak which could lower the strengths of the H α line. The measurement of the H α EW is not affected by calibration errors and very reliable in terms of its physical origin as it is directly related to the percentage of very young, blue stars in the region. We therefore assume that the population at the GRB site must be very young, not older than 7 M yr which is equal to the lifetime of a 30 solar mass star.

We also analyzed the burst region separately with photometry for the H II region of the GRB using an aperture of radius $0.4''$ and a sky annulus from 0.6 to $1''$. The small aperture was necessary since the GRB occurred in the spiral arm of the galaxy. All the images had similar see-

TABLE 2
Emission lines in different parts of the GRB 060505 host galaxy

Line	Site	obs [Å]	EW [Å]	F flux (measured) [10^{-17} erg/cm ² /s/Å]	Balmer abs. [10^{-17} erg/cm ² /s/Å]	F flux (corr.) [10^{-17} erg/cm ² /s/Å]
[O ii] 3727/29	GRB	4064.6	152.3	11.2 0.2		12.6 0.2
	Bu	4063.2	97.9	12.7 0.3		12.7 0.3
	Bm	4062.9	48.91	16.8 0.4		28.2 0.6
	Bl	4061.8	56.38	13.4 0.4		13.4 0.4
	ls	4061.5	43.83	2.87 0.08		2.87 0.08
H 4340	GRB	4731.6	9.82	1.12 0.02	0.70 0.01	2.02 0.02
	Bu	4730.5	6.85	1.45 0.03	1.70 0.02	3.15 0.04
	Bm	4731.0	1.796	0.99 0.03	3.79 0.03	7.33 0.18
	Bl	4729.4	2.598	0.86 0.03	3.24 0.03	4.10 0.04
	ls			< 0.04	0.77 0.01	< 0.77
H 4861	GRB	5299.9	39.20	2.98 0.02	0.57 0.01	3.88 0.02
	Bu	5298.3	27.22	4.53 0.02	1.81 0.02	6.34 0.03
	Bm	5297.1	8.064	4.27 0.03	3.80 0.03	11.9 0.05
	Bl	5296.3	12.60	3.35 0.02	2.90 0.03	6.25 0.04
	ls	5297.9	8.917	0.65 0.02	0.69 0.01	1.34 0.02
[O iii] 4959	GRB	5406.4	36.31	2.84 0.18		3.09 0.20
	Bu	5404.4	11.32	2.27 0.20		2.27 0.20
	Bm	5402.9	4.016	2.19 0.13		3.17 0.21
	Bl	5402.8	5.758	1.64 0.12		1.64 0.12
	ls	5403.4	6.004	0.43 0.03		0.43 0.03
[O iii] 5007	GRB	5458.6	92.80	7.20 0.06		7.85 0.06
	Bu	5456.4	40.46	7.84 0.14		7.84 0.14
	Bm	5456.3	9.709	5.17 0.13		7.50 0.18
	Bl	5455.1	17.70	4.85 0.13		4.85 0.13
	ls	5454.2	21.75	1.43 0.08		1.43 0.08
H 6567	GRB	7154.2	181.8	9.73 0.03	0.18 0.04	10.5 0.05
	Bu	7152.6	79.32	12.1 0.06	0.71 0.04	12.8 0.07
	Bm	7150.6	45.71	21.9 0.09	1.72 0.04	30.5 1.20
	Bl	7149.6	70.33	12.9 0.04	0.89 0.04	13.8 0.06
	ls	7150.1	34.70	1.59 0.02	0.21 0.03	1.70 0.04
[N ii] 6586	GRB	7175.8	19.44	0.96 0.03		1.02 0.03
	Bu	7174.5	16.45	2.53 0.06		2.53 0.06
	Bm	7172.7	10.62	4.97 0.09		6.43 0.11
	Bl	7172.3	13.08	2.28 0.04		2.28 0.04
	ls	7175.4	6.142	0.27 0.03		0.27 0.03
[S ii] 6716	GRB	7321.1	50.81	1.60 0.04		1.69 0.04
	Bu	7319.3	23.04	3.04 0.05		3.04 0.05
	Bm	7318.1	10.55	4.58 0.03		5.87 0.04
	Bl	7317.4	14.57	2.34 0.03		2.34 0.03
	ls	7316.2	29.42	0.77 0.12		0.77 0.12
[S ii] 6731	GRB	7335.6	36.25	1.09 0.04		1.15 0.04
	Bu	7334.4	20.25	2.64 0.05		2.64 0.05
	Bm	7332.7	7.164	3.10 0.03		3.97 0.04
	Bl	7331.9	9.370	1.48 0.03		1.48 0.03
	ls	7334.5	36.05	0.91 0.12		0.91 0.12

Note. | Abbreviations for the different parts along the slit: "GRB" = GRB explosion site, "bu" = upper part of the bulge, "bm" = middle part, "bl" = lower part, "ls" = lower spiral arm. Observed wavelengths are not corrected for the zero point error of around 4 Å mentioned in Chap. 3.2. Fluxes are corrected for the extinction at the GRB site of $E(B-V) = 0.03$ mag, underlying stellar absorption for the Balmer lines and the continuum had been corrected for the Galactic extinction of $E(B-V) = 0.021$ mag. The errors in the fluxes do not include the overall error from the flux calibration which might be around 10%

ing except for the I and Ks bands which were smoothened to the resolution of the BVR images before the photometry was extracted. A aperture corrections were determined from isolated well-exposed but non-saturated stars in the science images. The photometry was corrected for Galactic extinction. We did a similar analysis for the other H II region to the west of the GRB site in the same spiral arm which was outside the slit in order to investigate a possible connection between the two regions in terms of their ages. A summary of the photometry, zero points and de-

rived magnitudes and colors of these two H II regions are presented in Table 4. For the second H II region, the signal in the K band was too low to derive any magnitude.

In order to interpret the photometric results we compared our values to predictions from the spectral evolutionary synthesis models by Zackrisson et al. (2001). As our standard model we adopted an instantaneous burst with Salpeter IMF from 0.08 to 120 M_{sun} and a metallicity for the stars and gas of $Z = 0.004$. For the extinction we used a Galactic extinction law (Cardelli et al. 1989). The

TABLE 3
ISM properties in the different parts

Site	Pop. age [M yr]	M etall. (KD 02/Kewley07) 12+ log(O/H) or Z	SFR/8 pixel [M /yr]	M _B [M yr ⁻¹ L ⁻¹]	SSFR [M yr ⁻¹ L ⁻¹]	T _e [K]	extinction E (B-V)
GRB	< 7	8.26 (7.84) or 0.37 (0.14)	0.024	13.82	17	< 10,400	< 0.03
upper Bulge	640	8.97 (8.57) or 1.9 (0.76)	0.033	14.86	9.4	< 13,600	< 0.01
middle Bulge	800	8.99 (8.59) or 2.0 (0.79)	0.054	16.03	5.2	< 33,800	< 0.13
lower Bulge	286	9.00 (8.60) or 2.0 (0.81)	0.032	14.99	8.1	< 16,500	< 0.01
lower Spiral arm	128	8.97 (8.57) or 1.9 (0.76)	0.003	13.60	2.7	< 44,000	< 0.01

Note. | KD 02 and Kewley07 refer to Kewley & Dopita (2002) and Kewley et al. (2007)

TABLE 4
Photometry of the GRB site and the
nearby H II region west of the GRB site

F filter	GRB site [mag]	H II region [mag]
B	24.31	0.13
V	23.99	0.09
R	23.84	0.07
I	23.53	0.15
K	21.95	0.30

best fitting age and reddening were found to be 30–35 M yr and fitting E (B-V) to < 0.05. This extinction is very close to the value derived from the H₂/H ratio in the spectra. The modelling for the H II region west of the GRB site gave an even lower age of 3–5 M yr but at a higher extinction of E (B-V) = 0.25. Even though we lack a further proof of the age for this region from for example spectroscopic measurements of the H₂-EW or the correct extinction from the Balmer decrement, it suggests that these two H II regions are considerably different from the rest of the galaxy and that they might indeed have both been triggered at approximately the same time by a minor merging event as suggested in Sect. 3.1.

Another population model often used for GRB host galaxies is the population synthesis models from Bruzual & Charlot (2003). We use them to determine the age in the five parts of the 2D spectrum taking so called single stellar populations (SSP) models that are simply instantaneous starbursts. The assumed initial mass function is a Salpeter function with a lower cut-off of 0.1 M_⊙ and an upper cut-off of 100 M_⊙. For each of the 5 segments probed by the longslit we then determine the SSP model that fits the spectrum best, assuming both solar metallicity and a metallicity of Z = 0.004. We find a clear trend of decreasing age as a function of distance to the center of galaxy. In the center we find acceptable fits with ages in the range 300–800 M yr (depending on the metallicity), lower than the global value derived by the SED which might be due to the fact that we assume a single starburst for the bulge region which has very likely a more complex population. The youngest age is inferred for the GRB site where we infer an age of 47 M yr. In Fig. 5 we show two examples from the GRB site and the middle of the bulge as representation of the youngest and oldest populations.

The values derived from the modelling of the stellar continuum is generally higher than the one derived from the measurement of the H₂-EW. The models by Zackrisson et al. (2001) give slightly lower ages than the

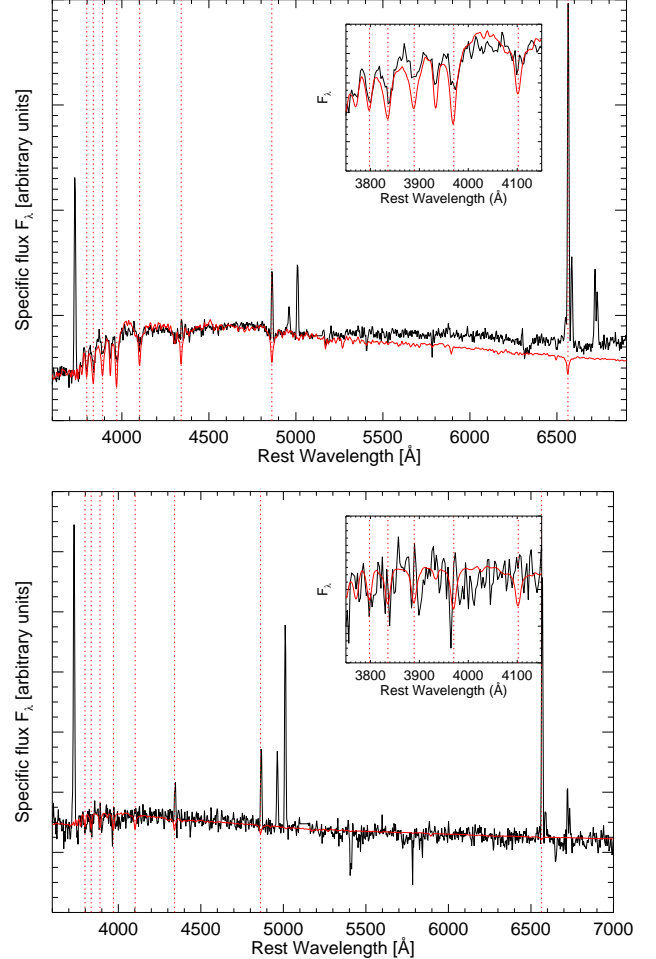


Fig. 5. | Examples for the population model fitting for the different regions in the galaxy (red) and the spectrum from that region (black). The upper figure is the galaxy spectrum at the GRB site (47 M yr), the lower one from the middle of the bulge (800 M yr). In the small insets, the blue part of the spectrum showing H_α, H_β and the stellar Ca H & K absorption is enlarged. One can see that the Balmer absorption for the population at the GRB site is smaller than expected from the model, a younger model, however, would give a too high excess in the blue. For the bulge model, however, it expects a higher flux in the blue in order to fit the red end which might point to an even older underlying population component.

Bruzual & Charlot (2003) models. The important difference between these two models is the inclusion of the nebular emission in the Zackrisson et al. (2001) models which is especially important at young ages. We also note that the HST images (O’Féak et al. 2007) reveal that

the burst site we identify as one H II region might in fact be a superposition of several different star-forming regions with different ages which might affect our analysis. As the two stellar continuum models are also dependent on calibration errors, we take the very low age of 7 M yrs from the H \rightarrow EW as the best reliable age for the H II region of the GRB site and assume that the GRB came from a 30 M \odot star. A further determination of a young age of the GRB region could be done by directly detecting the presence of Wolf-Rayet (WR) stars (Hammer et al. 2006; Wiersma et al. 2007). Unfortunately the flux limit of our spectrum is not sensitive enough to detect WR star lines. The young ages found for this region, however, connect well with predictions from the latest stellar evolution models for the lifetimes of massive, rapidly rotating, chemically homogeneous single star progenitors (Yoon & Langer 2005; Woosley & Heger 2005).

4.4. Metallicity

In order to determine the metallicity, we used the R_{23} parameter (first proposed by Page et al. 1979) which is a two-valued function of the metallicity. The degeneracy between the two solutions can be broken by using the ratio $[N\,ii]/H\alpha$ (Lilly et al. 2003) which in our case gives a clear preference for either the branch of low (GRB site) or high (bulge) metallicity. The metallicity, however, depends on the flux of the H α line which is usually affected by absorption from the underlying stellar population. Stellar population modelling (see Sect. 4.3), however, showed that the models and therefore the absorption in the Balmer lines needed for their correction depends only weakly on the metallicity, but mainly on the age of the population.

In the last years, a number of recalibrations of the R_{23} parameter have been done. Most of the recent metallicities of GRB host galaxies have been determined using the parametrization of Kewley & Dopita (2002) for the two branches which takes into account the oxygen ionization state. Using a first guess for the metallicity and a decision for the upper or lower branch solution, the metallicity then can be determined iteratively which usually converges very fast. Recently, a new recalibration has been done by Kewley et al. (2007) which corrects for the known overestimation of the metallicity from the R_{23} parameter. In the following, we give both the Kewley & Dopita (2002) values and the ones using the Kewley et al. (2007) correction.

The metallicity varies largely over the different regions in the host galaxy (see Table 3 and Fig. 4). In the star-forming region at the GRB site, the metallicity is relatively low with $12 + \log(O/H) = 8.26$ (7.84) which corresponds to 0.37 (0.14) Z \odot adopting the old (new) calibration and taking $12 + \log(O/H) = 8.69$ for the solar metallicity (Asplund et al. 2004). In the rest of the galaxy, the metallicity comes close or even above solar with values of $12 + \log(O/H) = 8.9$ (8.6) where we also have a much older stellar population which could be responsible for the enrichment of the ISM in that part of the galaxy. From these measurements, we can infer a (O/H) metallicity gradient throughout the galaxy of 0.08 dex kpc^{-1} .

An independent estimate for the metallicity comes from the so-called O3N2 method using the ra-

tio $O\,3N\,2 = \log((O\,iii/H\alpha)/[N\,ii/H\alpha])$ (e.g. Pettini et al. 2004), which is empirically calibrated on a sample of H II regions with electron temperature (T_e) determined in metallicities. Using the prescription of Pettini et al. (2004) we find an O3N2 determined metallicity estimate of $12 + \log(O/H) = 8.73 \pm 0.32$ O3N2 = 8.33 for the GRB region, which is similar to the estimate through the R_{23} method.

4.5. Relative SFR

The instantaneous star formation rate (SFR) can be obtained from the H α emission flux as H I is excited by UV light mainly coming from young, blue O stars which have their peak luminosity in the UV. The conversion formula for H α is then $\text{SFR} [M_\odot \text{yr}^{-1}] = 7.9 \cdot 10^{-42} \cdot 4 \cdot L [erg \text{s}^{-1}] d_L^2$ (Kennicutt 1998) where d_L the luminosity distance and L the H α line luminosity.

As we only cover a part of the galaxy by the slit, we cannot make a statement about the global SFR in this spiral galaxy, but only about the relative SFR between the different parts that we extracted from the spectrum. Table 3 lists the SFR per 8 \times 5 pixels along the slit (the area covered by the individual parts of the 2D spectrum) which corresponds to an area of $3.28 \times 2.05 \text{ kpc}^2$. At first look, we see that the current SFR seems to be much higher in the bulge and the innermost regions of the galaxy than at the GRB site, even though the population is much older there. One has, however, to take into account that the bulge contains more material than the spiral arms. We therefore scale the SFR with the B-band luminosity fraction compared to the luminosity of a "standard" galaxy of $M_B = -21$ mag (Christensen et al. 2004) to get the specific SFR for the individual regions. For the B-band magnitudes of the parts corresponding to the individual spectra, we determine the magnitude in a rectangular aperture of size 8 \times 5 pixels (9.5 for the lower spiral arm) from the VLT host image at the same position as the spectrum pieces. The result (see Table 3 and Fig. 4) is remarkable. The SSFR is a factor of 3 to 4 higher at the SF region around the GRB site with $17 \text{ M}_\odot \text{yr}^{-1} L=L^{-1}$, compared to the value in the bulge of around 5 to 9 $\text{M}_\odot \text{yr}^{-1} L=L^{-1}$ which is higher than in an average spiral galaxy (Kennicutt 1998) and a low value of $2.7 \text{ M}_\odot \text{yr}^{-1} L=L^{-1}$ in the lower spiral arm. The SSFR at the GRB site, however, is very well into the average value in GRB host galaxies of $9.7 \text{ M}_\odot \text{yr}^{-1} L=L^{-1}$ (Christensen et al. 2004). To determine an absolute value for the SFR is, however, difficult as the absolute flux calibration might not be fully reliable. In addition, the B-band of our galaxy is shifted slightly towards the V-band, so the absolute magnitude in rest-frame B-band would be higher and therefore the SSFR slightly lower.

4.6. Electron temperature and density

The detection of the [S ii] doublet lines at 6716, 6731 enables us to determine the electron density of the ISM in the different parts of the galaxy. According to the models (Osterbrock 1989) for $T = 10,000 \text{ K}$, a temperature consistent with the values found from the [O iii] 4363 upper limit, we get low electron densities throughout the galaxy. Very low values have also been found for three other GRBs (Wiersma et al. 2007; Thone et al. 2006b)

where the ratio of [O ii]/[S ii] = 3727/3729 was used for which a similar model has been derived by Osterbrock (1989).

To derive limits on the electron temperature in the intermediate temperature regions of the star-forming regions (see e.g. Izotov et al. 2006), we use the temperature sensitive ratio of nebular and auroral lines [O iii] (4959, 5008)/[O ii] (4363) (Osterbrock 1989), assuming that the electron density determined from the [S ii] doublet is the same for both the low and intermediate temperature regions of the H II regions (see e.g. Osterbrock 1989). The auroral [O iii]/[O ii] is not significantly detected in the spectrum, but we can derive a 3 upper limit for the line flux. From that we can derive upper limits for the electron temperature in the different host regions. For the GRB site, we find a value of T_e ([O iii]) = 10,400 K and much higher limits for the other locations in the host (see also Table 3 where 2 sigma limits on T_e ([O iii]) are shown). In comparison, the host of GRB 031203 had T_e ([O iii]) = 13,400 K, (Pochas et al. 2004).

We convert the 3 upper limit on T_e ([O iii]) of 10,400 K for the GRB region to a limit on T_e ([O ii]) and find T_e ([O ii]) = 10,200 K using the conversion for an intermediate metallicity from Izotov et al. (2006) as indicated by the R_{23} estimate. With these limits we can determine a lower limit for the oxygen abundance in the GRB region. We find ionic abundance limits of $O\text{ II}/H\text{ II}$ & 1.1×10^{-5} and $O\text{ III}/H\text{ II}$ & 6.6×10^{-5} . The excitation is likely too low for O IV to be important, so we find that the total oxygen abundance limit in the GRB region is O/H & 7.7×10^{-5} , or $12 + \log(O/H)$ & 7.9, which is consistent with the R_{23} oxygen abundance estimate.

5. THE LARGE SCALE STRUCTURE AROUND THE GRB HOST GALAXY

The fact that the field of GRB 060505 is covered by the 2dF survey (Colless et al. 2001) allows us to study the large scale structure around it.

The galactic environments of GRBs have so far not been studied much. At low redshifts Foley et al. (2006) studied the field of the host galaxy of GRB 980425, which was reported to be a member of a group. However, based on redshift measurements of the proposed group members, Foley et al. (2006) could establish that the host of GRB 980425 is an isolated dwarf galaxy. Levan et al. (2006) also proposed GRB 030115 to be connected to a cluster around $z = 2.5$ based on photometric redshifts. At redshifts $z \approx 2$ a few GRB fields have been studied using narrow band Lyman aging (Fynbo et al. 2002, 2003; Jakobsson et al. 2005). In all cases several other galaxies at the same redshift as the GRB host were identified, but it is not sure whether the galaxy densities in these fields are higher than in blank fields as no blank field studies have been carried out at similar redshifts. However, the density of Lyman emitters were found to be as high as in the fields around powerful radio sources that have been proposed to be forming proto-clusters, which would suggest that GRBs could reside in overdense fields at $z \approx 2$ (but note also that Romancini et al. 2004 argue for a low galaxy density in GRB host galaxy environments).

To study the environment of the GRB 060505 host galaxy we searched the 2dF database for all redshift measurements within a 2×2 field around the GRB 060505 host and with redshifts within $z = 0.004$ (about 1000 km s $^{-1}$ at the host galaxy redshift $z_{\text{host}} = 0.089$). In

Fig. 6 we show the field and the result is striking. In the GRB field there is a large filamentary overdensity of galaxies with redshifts in the range 0.089–0.093. The filament extends towards the south west from the galaxy cluster Abell 3837 at $z = 0.0896$ located at a distance of 40 arcmin on the sky (4 Mpc in projection) from the host. This suggests that the host galaxy of GRB 060505 lies in the foreground of the galaxy cluster and that it may be falling into the overdense region defined by the cluster and the filament extending out from it.

6. DISCUSSION AND CONCLUSIONS

The host galaxy of GRB 060505 is somewhat unusual for a long-duration GRB host in not being a young, star-forming dwarf galaxy, but a spiral galaxy of Hubble type Sbc with a generally older stellar population than found for GRB hosts. The galaxy might, however, have experienced a minor merger event in the recent past that could have triggered an episode of star formation in the northern parts of the galaxy, including the GRB site and another nearby young H II region.

The low redshift of the host galaxy of $z = 0.089$ puts us in the rare fortunate situation of allowing us to study the properties in the different parts of the galaxy in a spatially resolved longslit spectrum, including the star-forming region around the GRB site. The spatially resolved spectrum also enabled us to determine for the first time the rotation curve of a GRB host galaxy for which we find a maximum velocity of about 212 km s $^{-1}$.

Due to the 2dF survey, we were also able to study the galactic environment of the host galaxy. We found that it is located in the foreground of a filament stretching out from the Abell 3837 cluster at slightly higher redshift than the GRB host galaxy and suggest that it is falling towards this filamentary overdensity in the background.

The star-forming region around the burst site is shown to be largely different in its properties from the rest of the galaxy. Whereas the central parts of the galaxy contain an old population with a luminosity weighted age of 800 M yr, the burst site is connected to a SF region with a population of less than about 7 M yr. This is reflected by the current SFR scaled by the luminosity, being 3 to 4 times higher in the H II region that hosted the burst compared to the bulge. It is, however, similar to the global SFR found for other GRB host galaxies. Furthermore, the metallicity of the burst site is relatively low with only 0.14 Z $_{\odot}$ according to the most recent calibrations.

Connected to the nondetection of a SN in the lightcurve of GRB 060505, there has been some discussions about the classification of the burst as a long-duration GRB (O’Féak et al. 2007). In addition, some concerns were put forward that the association between the GRB and the low-redshift 2dF galaxy might be due to a chance superposition (Schaefer & Xian 2006). The clear association of the OT position with a star-forming region with an offset of $< 0.1^{\circ}$ or 40 pc, however, disfavours this possibility and strengthens the suggestion that GRB 060505 was due to the collapse of a massive star that originated in this star-forming region. A recent paper by O’Féak et al. (2007) uses the HST to obtain a high resolution, resolved in age of the star-forming region. They locate the afterglow to the outer part of the region, but the position of the afterglow is consistent with being in the centre of the star-forming region within 2 $^{\circ}$. Under the

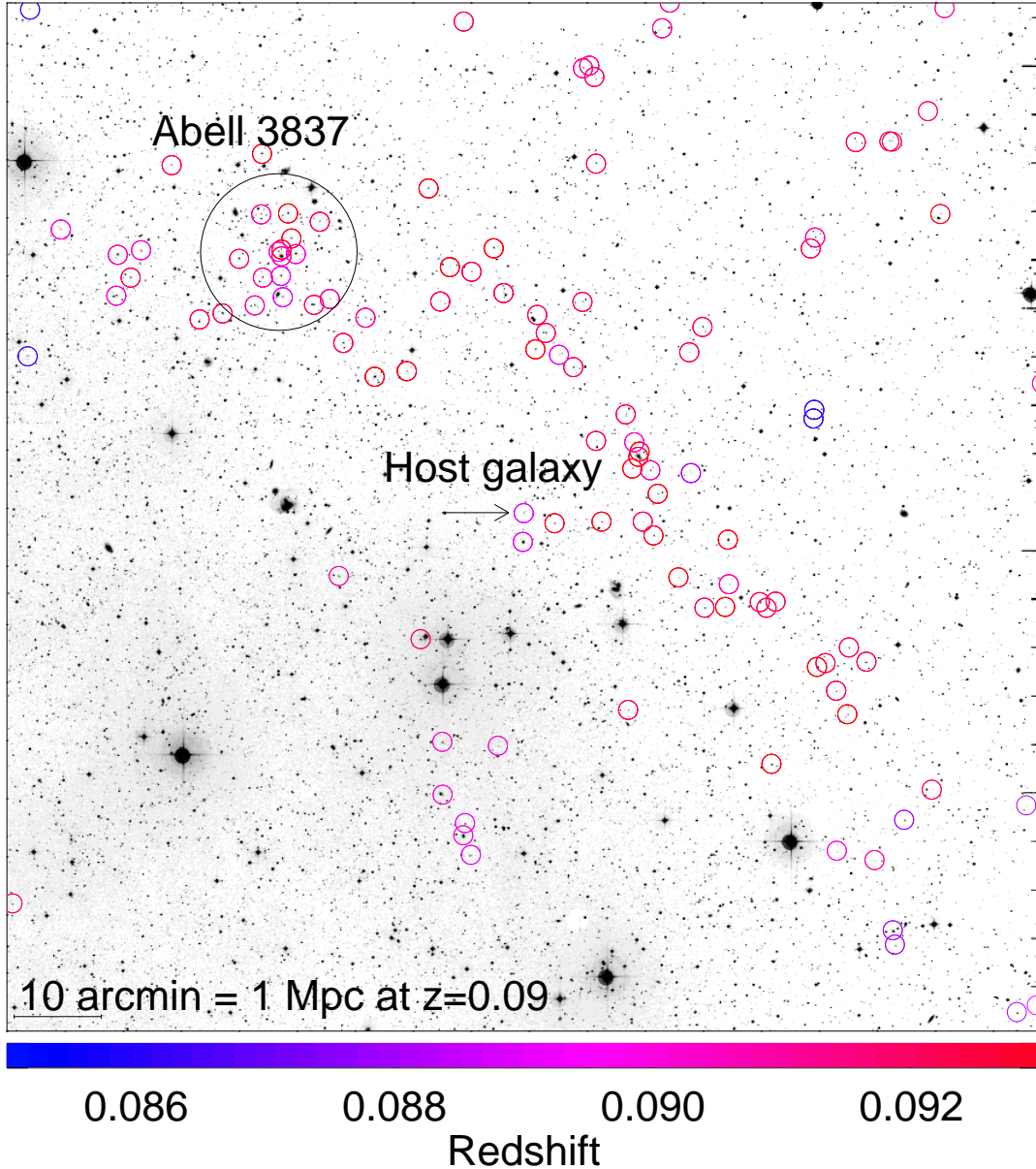


Fig. 6. The large scale structure around the host galaxy of GRB 060505 shown in a field of a size of 2×2 . The colored circles indicate the galaxies with redshifts known from the 2dF galaxy survey. Blue indicates galaxies with a lower redshift compared to the host galaxy, red a higher redshift. Most galaxies in the field lie on a filament at slightly higher redshift than the host galaxy, stretching out from the Abell 3837 cluster to the North-East of the host.

assumption that GRB 060505 was due to a merger event they derive a maximum age of 10 Myr for the progenitor system assuming the lowest possible kick-off velocity from their birth site which is consistent with the shortest time-delays of a merging system (Belczynski et al. 2006). One could however always argue in this direction as the birth sites of a possible merging system could have been anywhere in that galaxy and the clear association with a star-forming region speaks more in favour of a massive star progenitor.

O'leary et al. (2007) argues that the properties of the host galaxy and the location of the burst within its host is evidence that GRB 060505 is of a different nature than other long GRBs, in particular in comparison with the

sample in Fruchter et al. (2006). However, similar hosts and burst locations have been found for a few other long GRBs in contrast to what is stated in O'leary et al. (2007). In particular, the long-duration bursts GRB 980425 (Fynbo et al. 2000), GRB 990705 (Le Floc'h et al. 2002) and GRB 020819 (Jakobsson et al. 2005) were also located in the outer parts of spiral hosts. Fruchter et al. (2006) also argue that even though most GRB hosts are young, metal-poor dwarfs, long GRBs that are found in spiral galaxies would lie on the outskirts of those, preferring metal-poor, star-forming regions which is exactly the case for GRB 060505. O'leary et al. (2007) also notes the importance of measuring the metallicity of the burst site itself in order to get a clearer picture of whether

this burst could have a massive star progenitor.

Further support to the suggestion of a collapsar origin for that burst comes from the remarkably young age of the stellar population at the GRB site of below 7 M yr, which is just barely consistent with even the shortest timescales needed for a binary compact object system to merge (Belczynski et al. 2006). Also, there should be no reason to expect a low metallicity for a merging system. Even though some short-duration GRBs have occurred in star-forming galaxies (e.g. Fox et al. 2005; Covino et al. 2005; Soderberg et al. 2006) the specific star formation of the GRB 060505 H II region is significantly larger than that inferred for these events. Our arguments therefore strongly suggest that GRB 060505 was in fact the result of the death of a massive star as assumed for the origin of long-duration GRBs and that died without leaving a

SN for which the reason is currently not known.

We thank the observers and the Paranal staff for performing the observations reported in this paper. B.M.-J. wants to thank Steven Bamford for valuable discussions about rotation curve fitting of well resolved galaxies. G.O. thanks E. Zackrisson for explanations on his stellar population synthesis code. The Dark Cosmology Centre is funded by the Danish National Research Foundation. K.W. thanks NW0 for support under grant 639.043.302. D.M. acknowledges support from the Instrument Center for Danish Astrophysics. J.G. is supported by the Spanish research program M.S.ESPA 2004-01515 and E.S.P. 2005-07714-C 03-03.

REFERENCES

A splund, M., Greville, N., Sauval, A. J., Alende Prieto, C. & Kiselman, D. 2004, *A & A*, 417, 751
 Belczynski, K., Perna, R., Bulik, T., Kalogera, V., Ivanova, N. & Lamb, D. Q. 2006, *ApJ*, 648, 1110
 Bertin, E. & Arnouts, S. 2006, *A & A S*, 117, 393
 Biviano, A. & Girardi, M. 2003, *ApJ*, 585, 205
 Blanton, M. R. et al. 2001, *AJ*, 121, 2358
 Bolzonella, M., Miralles, J.-M. & Pello, R. 2000, *A & A*, 363, 476
 Bomancini, C. G., Martínez, H. J., Lambas, D. G., Le Floc'h, E., Mirabel, I. F. & Minniti, D. 2004, *ApJ*, 614, 84
 Bruzual, G. & Charlot, S. 2003, *MNRAS*, 344, 1000
 Butler, N. R. 2007, *AJ*, 133, 1027
 Cardelli, J. A., Clayton, G. C. & Mathis, J. S. 1989, *ApJ*, 345, 245
 Christensen, L., Hjorth, J. & Gorosabel, J. 2004, *A & A*, 425, 913
 Colless, M. et al., 2001, *MNRAS* 328, 1039
 Cencio, M. L., Capalbi, M., Vettore, L., Palmer, D. & Burrows, D. 2006, *GCN circ.* 5115
 Covino, S. et al. 2006, *A & A*, 447, L5
 Della Valle, M. et al. 2006, *Nature*, 444, 1050
 Le Floc'h, E., Duc, P.-A., Mirabel, I. F., Sanders, D. B., Bosch, G., Rodriguez, I., Courvoisier, T. J.-L., Mereghetti, S. & Melnick, J. 2002, *ApJ*, 581, L81
 Le Floc'h, E. et al. 2003, *A & A*, 400, 499
 Le Floc'h, E., Chamaillard, V., Forrest, W. J., Mirabel, I. F., Armus, L. & Devost, D. 2006, *ApJ*, 642, 636
 Foley, S., Watson, D., Gorosabel, J., Fynbo, J. P. U., Solleman, J., McGlynn, S., McBreer, B. & Hjorth, J. 2006, *A & A*, 447, 891
 Fox, D. B. et al. 2005, *Nature*, 437, 845
 Fruchter, A. S. et al. 2006, *Nature*, 441, 463
 Fryer, C. L., Young, P. A. & Hungerford, A. L. 2006, *ApJ*, 650, 1028
 Fynbo, J. P. U. et al. 2000, *ApJ*, 542, L89
 Fynbo, J. P. U. et al. 2002, *A & A*, 388, 425
 Fynbo, J. P. U. et al. 2003, *A & A*, 406, L63
 Fynbo, J. P. U. et al. 2006, *Nature*, 444, 1047
 Fukugita, M., Shimada, K. & Ichikawa, T. 1995, *Publications of the Astronomical Society of the Pacific*, 107, 945
 Gal-Yam, A. et al. 2006, *Nature*, 444, 1053
 Garnett, D. R., Shields, G. A., Sklaman, E. D., Sagan, S. P. & Dufour, R. J. 1997, *ApJ* 489, 63
 Gehrels, N. et al. 2004, *ApJ* 611, 1005
 Gehrels, N. et al. 2006, *Nature*, 444, 1044
 Hammar, F., Flores, H., Schaefer, D., Dessauges-Zavadsky, M., Le Floc'h, E. & Puech, M. 2006, *A & A*, 454, 103
 Hjorth, J. et al. 2003, *Nature*, 423, 847
 Hullinger, D. et al. 2006, *GCN circ.* 5142
 Izotov, Y. I., Stasinska, G., Meynet, G., Guseva, N. G. & Thuan, T. X. 2006, *A & A*, 448, 955
 Jakobsson, P. et al. 2005, *ApJ*, 629, 45
 Kaumann, G. et al. 2003, *MNRAS*, 346, 1055
 Kennicutt, R. C. Jr. 1992, *ApJS*, 79, 255
 Kennicutt, R. C. Jr. 1992, *ApJ*, 388, 310
 Kennicutt, R. C. Jr. 1998, *ARA & A*, 36, 189
 Kewley, L. & Dopita 2002, *ApJS*, 142, 35
 Kewley et al. 2007
 King, A., Olszon, E. & Davies, M. B. 2007, *MNRAS*, 374, 34
 Levan, A. et al. 2006, *ApJ*, 647, 471
 Lilly, S. J., Carollo, C. M. & Stockton, A. N. 2003, *ApJ*, 597, 730
 Michalowski, M. J. & Hjorth, J. 2007, *A&P*, Proceedings of the Cefalu Conference, in press
 Ofelek, E. O., Cenko, S. B., Gal-Yam, A., Peterson, B., Schmidt, B. P., Fox, D. B. & Price, P. A. 2006, *GCN circ.* 5123
 Ofelek, E. O. et al. 2007, *ApJ*, submitted (astro-ph/0703192)
 Osterbrock, D. E. 1989, *Astrophysics of Gaseous Nebulae and Active Galactic Nuclei*, University Science Books, Mill Valley, CA
 Pagel, B. E. J., Edmunds, M. G., Blackwell, D. E., Chun, M. S. & Smith, G. 1979, *MNRAS*, 189, 95
 Palmer, D., Cummins, J., Stamatis, M., Markwardt, C. & Sakamoto, T. 2006, *GCN circ.* 5076
 Pettini & Pagel 2004, *MNRAS*, 348, L59
 Prochaska, J. X. et al. 2004, *ApJ*, 611, 200
 Schaefer, B. E. & Xiao, L. 2006, *ApJ*, submitted (astro-ph/0608441)
 Schlegel, D. J., Finkbeiner, D. P., & Davis, M. 1998, *ApJS*, 80, 1
 Solleman, J. et al. 2002, *A & A*, 386, 944
 Solleman, J., Ostlin, G., Fynbo, J. P. U., Hjorth, J., Fruchter, A. & Pedersen, K. 2005, *New Astronomy*, 11, 103
 Soderberg, A. M. et al. 2006, *ApJ*, 650, 261
 Stanek, K. Z. et al. 2003, *ApJ*, 591, L17
 Thone, C. C., Fynbo, J. P. U., Solleman, J., Jensen, B. L., Hjorth, J., Jakobsson, P. & Klose, S. 2006, *GCN circ.* 5161
 Thone, C. C., Greiner, J., Savaglio, S. & Jehin, E. 2006, *ApJ*, submitted (astro-ph/0711772)
 Voss, R. & Tauris, T. M. 2003, *MNRAS*, 342, 1169
 Wiersema, K. et al. 2007, *A & A*, 464, 529
 Woosley, S. E. & Heger, A. 2005, in *ASP Conf. Ser.* 332, "The Fate of the Most Massive Stars", ed. R. Humphreys & K. Stanek (San Francisco) p 407
 Yoon, S.-C. & Langer, N. 2005, *A & A*, 443, 643
 Zackrisson, E., Bergvall, N., Olofsson, K. & Siebert, A. 2001, *A & A*, 375, 814
 Zeh, A., Klose, S., & Hartmann, D. H. 2004, *ApJ*, 609, 952
 Zhang, B., Zhang, B. B., Liang, E.-W., Gehrels, N., Burrows, D. N., & Eszteros, P. 2007, *ApJ*, 655, L25